THE ASTROPHYSICAL JOURNAL, 452:401–406, 1995 October 10

THE RADIAL VELOCITY VARIABILITY OF α PERSEI: A LOW-AMPLITUDE CEPHEID OUTSIDE THE INSTABILITY STRIP?

ARTIE P. HATZES AND WILLIAM D. COCHRAN
McDonald Observatory, University of Texas at Austin, Austin, TX 78712
Received 1995 January 10; accepted 1995 April 20

ABSTRACT

Precise radial velocity measurements ($\sigma \sim 35$ m s^{-1}) are presented for the F5 supergiant α Per. Low-amplitude variations with a $2K$ amplitude of 300 m s^{-1} and a period of 87.7 days, or a possible (but less likely) period of 9.80 days, are detected. The favored period of 87.7 days most likely arises from rotational modulation by surface features or nonradial pulsations. If the radial velocity variations of α Per result from pulsations, then this star may represent a case for Cepheid-like pulsations in a star just outside of the known boundary of the Cepheid instability strip.

Subject headings: stars: individual (α Persei) — stars: oscillations

1. INTRODUCTION

Stellar pulsation is a pervasive phenomenon found in stars covering a wide range of spectral types: Cepheids, δ Scuti, rapidly oscillating Ap stars, B stars, white dwarfs, and the Sun. It could be argued that give sensitive enough detection techniques virtually all stars will be found to pulsate at some level or another. Recent advances in techniques for measuring stellar radial velocities (RVs) have reduced the error of these measurements from 200–500 m s^{-1} to 10–20 m s^{-1}. As expected, these high-precision measurements are discovering low-amplitude variability in stars previously thought to be constant. An excellent example of this are the K giants, several of which have recently been shown to be low-amplitude RV variables (Smith, McMillan, & Merline 1987; Walker et al. 1989; Hatzes & Cochran 1993, 1994a, b).

The Cepheids are perhaps the most famous class of pulsating stars. These objects are mostly supergiants (luminosity class Ib) occupying a narrow region in the H-R diagram commonly referred to as the instability strip. The precise boundaries of this strip are poorly known. Pulsating stars just outside of the instability strip may be common but as yet undetected, possibly due to the low amplitude of the pulsations. Furthermore, a star's residence inside the Cepheid instability strip is no guarantee that it is pulsating. At least half of the stars inside this region are stable down to a level of 0.01–0.03 mag in V (Fernie & Hube 1971; Percy 1975; Fernie 1976; Percy, Baskerville, & Trevorrow 1979). Recently, Butler (1992) presented precise RV measurements of the non-Cepheid F8 supergiant γ Cyg (= HR 7796) which showed variability with a peak-to-peak ($2K$) amplitude of 350 m s^{-1} and a period of 11.867 days. He proposed that this star was, in fact, an extremely low amplitude Cepheid.

Finding other examples of low-amplitude Cepheids may help define the true boundary of the instability strip as well as provide a better understanding of the mechanism that makes a star a Cepheid variable. The star α Per is an F5 supergiant whose M_V and $B-V$ values (Humphreys 1978) suggest that it lies just outside the theoretical blue edge of the instability strip (see Fig. 10 below). This star was included as part of a program to measure the RV variations in a sample of K giants. In this paper, RV measurements of α Per are presented and it is shown that this star is a low-amplitude variable and possibly a pulsating star.

2. OBSERVATIONS AND RESULTS

2.1. *Data Acquisition*

Observations of α Per were made from 1991 October to 1993 August using the coudé spectrograph of the McDonald Observatory 2.1 m telescope. High RV precision was achieved by placing a molecular iodine gas absorption cell in front of the entrance slit to the spectrograph during a stellar observation. The iodine spectrum provides a stable wavelength reference for measuring RVs (Marcy & Butler 1992; Libbrecht 1988; Cochran & Hatzes 1994). The instrumental setup is the same one employed in our K giant RV survey. This consisted of a 1200 gr mm^{-1} grating used in second order along with a Tektronics 512 × 512 CCD. The instrumental resolution was of 0.11 Å (2.4 pixels) centered on 5520 Å. A description of the RV data reduction can be found in Hatzes & Cochran (1993). Extensive use of the iodine cell with this instrumental setup indicates that for cool stars rich in stellar lines a long-term (month-to-month) RV precision of 20–25 m s^{-1} is possible.

Each night up to four individual observations of α Per were made. The RV measurements from these data were averaged to produce the nightly means listed in Table 1. Figure 1 is a plot of the tabulated RV values.

2.2. *Period Analysis*

A period analysis of the data was performed using three techniques: a Scargle-type periodogram (Scargle 1982), the CLEAN algorithm of Roberts, Lehár, & Dreher (1987), and a least-squares sine-fitting procedure.

Figure 2 shows the Scargle-type periodogram on the nightly means of the RV measurements as well as the window function. The highest peak occurs at a frequency of 0.0114 day^{-1} ($P = 87.7$ days) and has a false-alarm probability of 0.2%. There is a secondary peak at $\nu = 0.102$ day^{-1} ($P = 9.805$ days).

The CLEAN algorithm of Roberts et al. (1987) is designed to remove artifacts introduced into the data power spectrum by the sampling window. The upper panel of Figure 3 shows the "dirty" Fourier transform of the data with the effects of the observation window present. The lower panel shows the CLEANed transform. In both panels the dominant peak occurs at $\nu = 0.102$ day^{-1}. The secondary peaks in the CLEANed transform are not considered to be significant. It is puzzling that the dirty transform does not have significant power at 0.0114 day^{-1}, the dominant peak in the Scargle

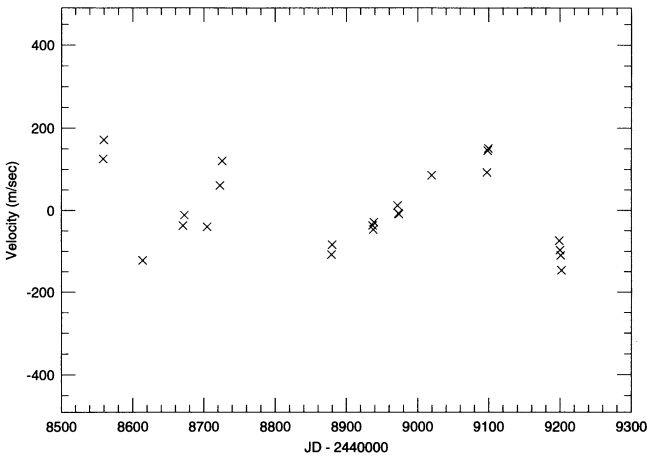

FIG. 1.—Relative RVs of α Per from 1991 October to 1993 August

periodogram. It has been our experience in extensive use of both techniques that structure found in periodograms can generally be identified with features in the Fourier power spectrum.

Finally, a period search was performed on the data by fitting sine functions to the RV data. Figure 4 shows the reduced χ^2 of the fits as a function of the frequency of the least-squares sine wave. The χ^2 is minimized at $\nu = 0.0115$ day^{-1} ($P = 87.0$ days),

TABLE 1

α PER RELATIVE RVs (NIGHTLY AVERAGES)

Date[a]	V (m s^{-1})	Date[a]	V (m s^{-1})
8,558.861.....	125.6	8,938.784.....	−29.2
8,559.826.....	171.6	8,971.646.....	11.6
8,613.815.....	−122.4	8,972.891.....	−7.4
8,670.689.....	−37.4	8.973.638.....	−9.3
8,672.703.....	−11.6	9.019.666.....	85.6
8,704.583.....	−40.4	9,097.614.....	92.6
8,722.591.....	60.6	9,098.612.....	145.3
8,725.593.....	120.7	9,099.611.....	150.6
8,878.939.....	−108.6	9,198.952.....	−74.4
8,879.950.....	−84.4	9,199.958.....	−97.4
8.936.875.....	−37.4	9,200.968.....	−110.4
8,937.820.....	−47.4	9,201.956.....	−147.1

[a] Date = Julian Day −2,440,000.0.

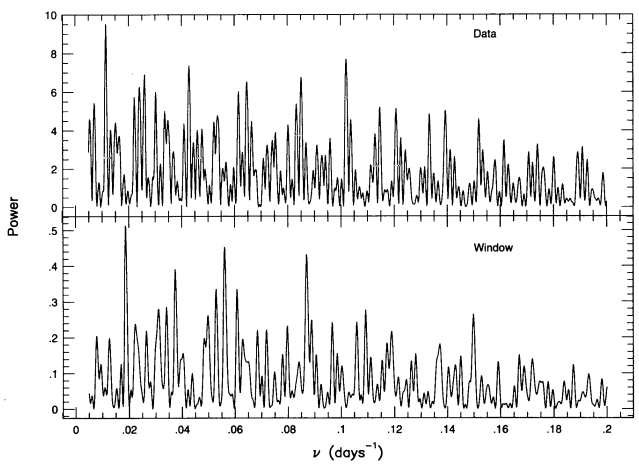

FIG. 2.—*Upper*, Scargle-type periodogram of the nightly averages of the RV data presented in Fig. 2. *Lower*, Window function.

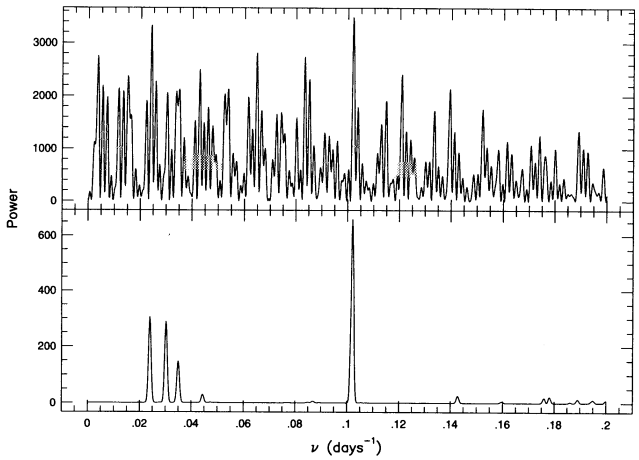

FIG. 3.—*Upper*, "Dirty" Fourier transform of the nightly averages of the RV measurements for α Per. *Lower*, Fourier transform after application of the CLEAN algorithm.

and there is a secondary minimum at $\nu = 0.102$ day^{-1}. These results are consistent with the Scargle-type periodogram analysis.

Figure 5 shows the phase diagram using the primary and secondary periods from the periodograms. Both periods result in obvious sinusoidal variations, although the scatter about the mean curve for the 87.7 day period ($\sigma \approx 35$ ms^{-1}) is smaller than that for the 9.8 day period ($\sigma \approx 50$ m s^{-1}).

The scatter of the phase diagram for the 87.7 day period seems to be more consistent with the expected errors of the RV measurements. The RV precision for K giants in this program is about 20–25 m s^{-1}. This precision, however, depends on the number, depth, and width of spectral lines used in computing the RV. The cool K giants tend to be slow rotators with a plethora of lines, whereas the spectrum of α Per has fewer lines that are broadened by appreciable stellar rotation. The rms scatter of the nightly RV measurements for α Per range from 20 to 55 m s^{-1} and with an average of about 30 m s^{-1}. This, however, only indicates the short-term precision, and the long-term error can be significantly larger. To estimate these errors, 10 observations of α Per (taken without the iodine cell) were co-added to produce a high signal-to-noise (S/N > 800) spectrum that was used as a model. A barycentric shift was applied

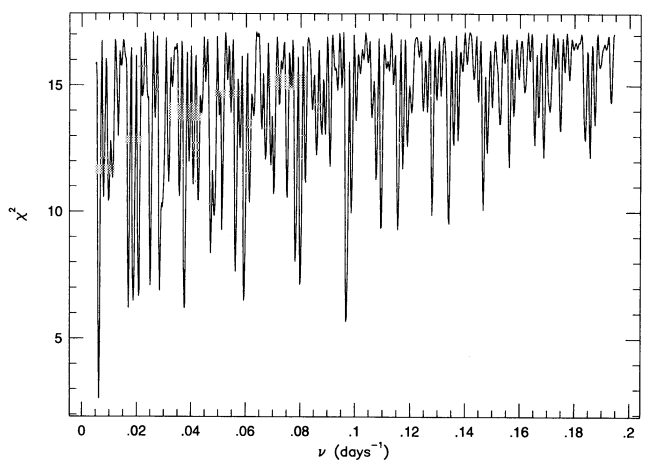

FIG. 4.—Reduced χ^2 as a function of input sine frequency for the least-squares sine-fitting procedure.

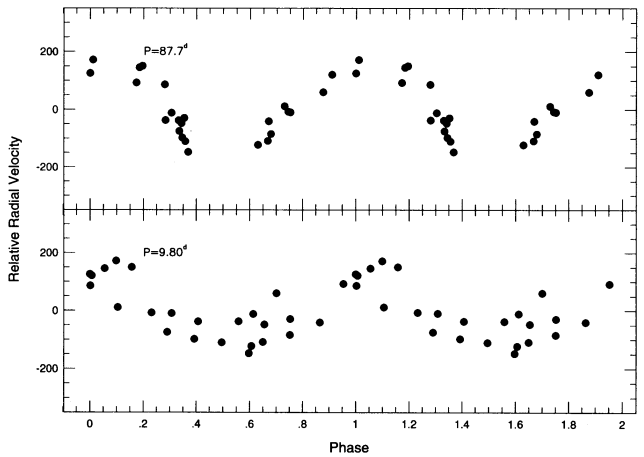

FIG. 5.—*Upper*, RVs of α Per phased to a period of 87.7 days. *Lower*, Variations phased to the 9.80 day period.

to the data as well as a slightly different dispersion to mimic observing the star at different times of the year. This stellar spectrum was then combined with a high signal-to-noise (S/N > 500) spectrum of pure molecular iodine. Random noise at a level of S/N = 300 (typical for the observational data) was also added. The rms scatter of the RV computed from a series of such synthetic data was about 60 m s^{-1}. Since three to four measurements are typically used in computing the nightly means, one expects the nightly averages to have a $\sigma \sim 30$ m s^{-1}, consistent with the scatter for the 87.7 day period.

Changes in the instrumental point-spread function (PSF) can account for systematic errors from run to run, especially since the iodine absorption lines are unresolved at the resolution of the observations. In order to monitor the long-term systematic errors, the same region of the lunar surface was observed as a RV "standard." Figure 6 shows the RV measurements of the lunar spectra acquired over the same time span as the α Per observations. The standard deviation about the mean is 20 m s^{-1}. (The $\pm 1\ \sigma$ is shown by the dashed line.) There appear to be some slight systematic trends, but these are well within the $\pm 1\ \sigma$ bounds. Of course the Moon does not exactly mimic a stellar object as lunar light completely fills the slit, and this provides a different illumination of the spectrograph optics. Also there are minimal guide errors associated with the lunar observations. However, the slit width of the instrumental setup is 0.″5, which is considerably smaller than the typical seeing at the time of the observations (1.″5–2″). So, at least in one dimension, stars do provide a more or less uniform illumination of the slit, much as the Moon does. Exposure times of the Moon were comparable to those of the α Per observations, so Figure 6 probably represents a reasonably good measure of the RV errors resulting from changes in the PSF.

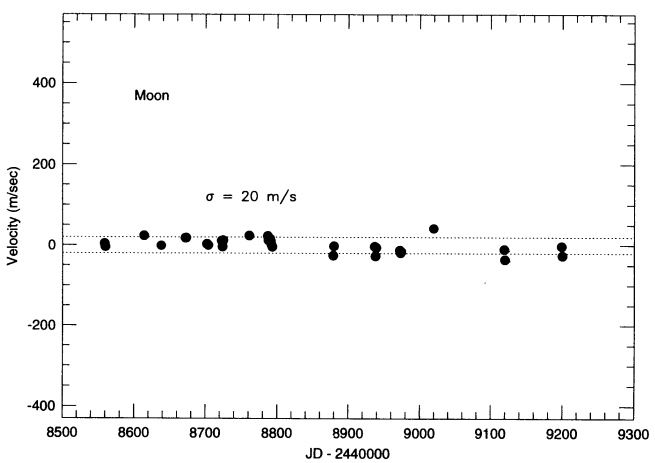

FIG. 6.—Relative RV measurements of the Moon. The dashed lines mark $\pm 1\ \sigma$.

As a further check of the stability of the PSF, emission spectra of hollow cathode lamps taken on the same nights as the α Per observations were examined. The spectra showed emission profiles that were consistently symmetric and whose FWHM from run to run varied by no more than about 4%. (On one night the FWHM of thorium lines was 10% above the mean value.) Figure 7 shows the measured RVs for α Per as a function of the change in the PSF. This change was quantified by the difference of the observed FWHM of thorium emission lines minus the mean FWHM over the entire span of observations. There is no obvious correlation of radial velocity with changes in the FWHM of the PSF.

2.3. *Numerical Simulations*

The prescription of Scargle (1982) for calculating the false-alarm probability is at best only an estimate of the statistical significance for a period detection. A better way to assess this statistical significance is via numerical simulations. A series of 1000 periodograms were generated from random noise with $\sigma = 50$ m s^{-1} and sampled in the same manner as the data. Figure 8 summarizes the results of these simulations.

The upper panel shows the histogram of the power values for the highest peak in the noise periodograms, expressed as a percentage of the numerical runs. In no instance did a noise periodogram have a peak with a power value greater than $P = 7.6$, significantly lower than the peak value of Figure 2. This indicates that the false-alarm probability for the 87.7 day period is less than 0.001, consistent with the initial low estimate of this probability.

It is possible for purely random noise to show structure in the data periodogram just from the sampling pathology. To investigate this, a histogram of the frequency of the maximum peak in the noise periodograms was also computed and this is shown in the lower panel of Figure 8. It is essentially flat, indicating that none of the major peaks in the data periodo-

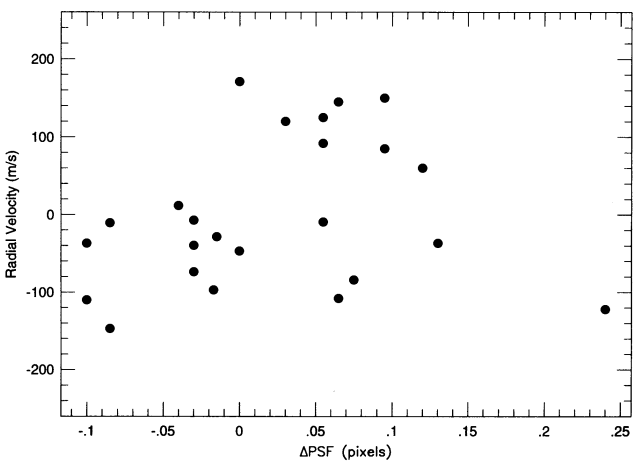

FIG. 7.—Measured RVs of α Per as a function of the change in instrumental PSF from run to run. The change in PSF was quantified by the difference between the FWHM of thorium emission lines at the time of the observations and the mean of the FWHM of such lines from all nights.

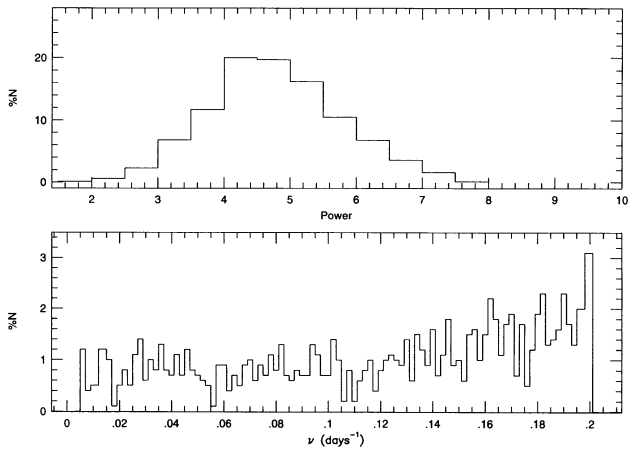

FIG. 8.—Results of Monte Carlo simulations on random noise with $\sigma = 50$ m s^{-1} and sampled in the same manner as the RV measurements. *Upper*, Histogram (in percentages of the number of numerical runs) of the peak values in the noise periodograms. *Lower*, Histogram of the frequency for the dominant peak in the noise periodograms.

gram can merely arise from the sampling pathology of pure noise.

To assess whether the 87.7 or 9.8 day period is most likely present, simulations were conducted using model data consisting of sine functions with these two periods and appropriate amplitudes (in the least-squares sense) that were sampled in the same manner as the real data. Noise with $\sigma = 50$ m s^{-1} was also added. In all cases (using 400 simulations) the Scargle periodogram and the CLEAN algorithm produced a dominant peak in the power spectrum that was coincident with the input period. This indicates that the highest peak in the data periodogram should represent the true period that is present.

In the case of the 9.8 day period it was impossible to produce significant power (secondary peak) at a period of 87.7 days. This is demonstrated in Figure 9, which shows the periodograms of pure sine waves with periods of 87.7 days (*upper panel*) and 9.8 days (*lower panel*) that had the same sampling pathology as the observational data. The periodogram of the 9.8 day synthetic data shows virtually no power near $\nu = 0.0114$ day^{-1}. Note how the periodogram of the 87.7 day period looks qualitatively similar to the real data periodogram (Fig. 2). There is a primary peak at $\nu = 0.0114$ day^{-1} and a

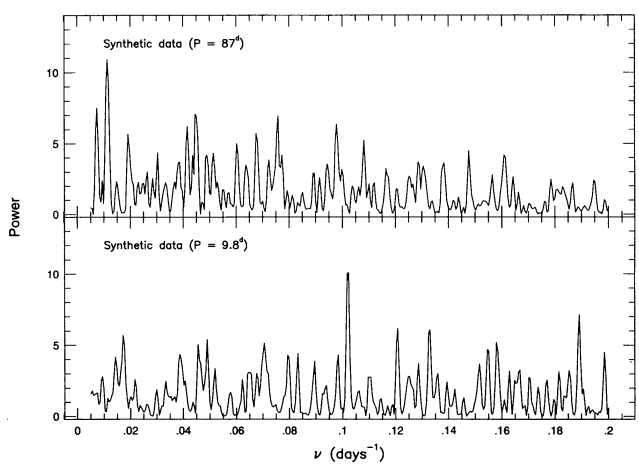

FIG. 9.—Scargle periodograms for synthetic data consisting of sine functions sampled in the same manner as the data. *Upper*, Periodogram for a 87 day sine wave. *Lower*, Periodogram for a 9.80 day sine wave.

secondary one near $\nu = 0.1$ day^{-1}, although this is shifted slightly to lower frequency than the analogous peak in the data periodogram. This may be due to RV variations departing from a true sine function. The phase diagram for the 87.7 day period (Fig. 5, *upper panel*) indeed shows a descending branch steeper than the ascending branch.

Although the 9.8 day period cannot be conclusively ruled out, the smaller scatter of the 87 day period phase diagram and the fact that a pure sine wave of this period seems to provide a good match, qualitatively, to the observed periodogram suggests that the longer period is the one that is present. The 9.8 day period cannot be conclusively ruled out, but it is short enough that its presence could easily be confirmed by one long observing run.

3. DISCUSSION

The interpretation of the RV variations depends to some extent on whether the 87.7 day or the 9.8 day period is actually present. Assuming that the preferred period of 87 days is the true one, then it can arise from either (1) a low-mass companion, (2) rotational modulation by surface features, or (3) stellar pulsations.

An orbit solution to the RV data yields a minimum mass function of $4.7 \times 10^{-8}\ M_\odot$. Parsons & Bouw (1971) list the mass and radius of α Per as 7.2 $M_\odot$ and 63 $R_\odot$, respectively. This yields a companion mass of $\sim$13 Jupiter masses and an orbital radius of 0.75 AU. The stellar radius (= 0.3 AU) thus represents a significant fraction of the orbital radius. It is not clear whether a gaseous, Jovian-type planet can form and survive so close to the stellar surface. If the planet is rocky, then its mass would be considerably larger than the combined mass of the terrestrial planets. Unfortunately the lack of observational evidence for extrasolar planetary systems prevents us from drawing any firm conclusions about the existence of a massive planet in a close orbit around an F supergiant. Although it cannot be completely ruled out, the low-mass companion hypothesis, at the present time, seems unlikely.

An alternative explanation for the long RV period is that it is due to a surface feature that modulates the RV with the same period as the star's rotation. These surface features can be any one of a number of phenomena that have been detected on other stars: dark spots, abundance anomaly patches, plagelike regions, or large convection cells, to name a few. Starspot activity in particular seems to be a common phenomenon among stars with deep convection zones and appreciable stellar rotation rates, so these features may well be present on α Per.

Dinshaw et al. (1989) found evidence for a 45 day period in the RV measurements of the Cepheid star Polaris and suggested that it may be due to a surface feature. If the RV variations were caused by a dark starspot then only about 2% of the stellar flux would have to be removed. Numerical stimulations indicate that a spot of radius $\approx 7°$ near the equator and having a temperature 1200 K below the photosphere (typical for starspots on RS CVn stars and sunspots) can produce an RV variation of ± 200 m s^{-1}. Such a spot is small enough that the spectral distortions in the spectral line profile would be only $\approx 1\%$.

To test whether rotational modulation is consistent with an 87 day period, the stellar rotation period was estimated using the projected rotational velocity ($v \sin i$) and the stellar radius determination of Parsons & Bouw (1971). The $v \sin i$ was measured using several weak spectral lines and a numerical inte-

gration of a stellar disk divided into 200 × 200 cells, each containing a local line profile generated using Kurucz's model atmospheres (Kurucz 1979). The best fit to the line profiles was provided by a $v \sin i$ of 18 km s^{-1} and a macroturbulent velocity of 10 km s^{-1}. This results in an upper limit to the rotation period of about 190 days (assuming a stellar inclination of 90°).

The true equatorial velocity of α Per is almost certainly higher than the measured $v \sin i$. A rotation period of 87 days implies an equatorial rotational velocity of 36 km s^{-1}, which would place α Per among the most rapidly rotating F supergiants. Danzinger & Faber (1972) included 16 F supergiant stars in their study of rotational velocities of evolved stars. The mean projected rotational velocity of this small sample was 15 km s^{-1}, and the largest value was 30 km s^{-1}. Assuming the latter as representing the true equatorial rotation for an F supergiant results in a stellar inclination for α Per of 40°. This gives a rotation period of 115 days, certainly in the range of the observed period. Also, the presence of two surface features separated by 180° could also result in a detected period of ≈90 days. So it is possible for surface features to account for an 87.7 day period in the RV variations. If so, then these features would have to be long lived and stable (i.e., nonmigrating) since the RV variations seem to be coherent over the 1 yr span of the observations. Independent confirmation of such dark features could come from multicolor photometric monitoring of this star or an examination of spectral lines that are indicators of activity or that are sensitive to temperature changes. Percy & Welch (1981) did observed α Per eight times in 10 nights and found no variation above about 0.02 mag in *b* and *y*, but possibly they observed the star when no "spot" was present.

The final possibility is that the 87 day period results from stellar pulsations. The fundamental radial mode is estimated to be about ~7 days, so the pulsations would have to be nonradial in nature. Nonradial pulsations are believed to be present in a few Cepheid stars; the period ratio of a few bump Cepheids have values of 0.8–0.9 (e.g., Antonello, Mantegazza, & Poretti 1986), and these have been attributed to nonradial pulsations. Perhaps the 87 day period of α Per and 45 day period seen in Polaris may represent similar nonradial pulsation modes.

Interestingly, if the 9.8 day period is actually present, then α Per behaves like a normal Cepheid star, albeit with extremely low amplitude. The period luminosity (*P-L*) relationship of Cepheids given by Kraft (1961) results in a predicted absolute visual magnitude, M_V, of −4.2 for α Per. The literature values of M_V for this star are −4.3 (Allen 1973), −4.5 ± 0.2 (Harris 1976), and −4.7 (Humphreys 1978). There are corrections to the period-luminosity relationship due to abundances (Eggen 1985a), but these amount to only about 0.1 mag or less.

The only known example of a extremely low amplitude Cepheid, γ Cyg (HR 7796), has a comparable amplitude ($2K \sim 100$ m s^{-1}) which is at least an order of magnitude less than the smallest amplitude Cepheid. If α Per has a 9.8 day period, then it and γ Cyg have comparable periods which, as pointed out by Butler (1992), are greater than the 4–8 day periods of small-amplitude Cepheids (Eggen 1985b). Unlike γ Cyg, whose velocity curve rises for about 75% of the pulsation cycle and then rapidly falls, the RV curve for α Per (Fig. 5, *lower panel*) appears to have a smooth sinusoidally varying RV curve, much like the small-amplitude Cepheids.

The ratio of the RV amplitude to photometric amplitude ($2K/\Delta V$) for classical Cepheids is 54 km s^{-1} mag^{-1} (Allen 1973). If α Per obeys this relationship, then the expected *V* amplitude should be about 0.004 mag. Integrating the RV curve for α Per yields radius changes of 0.06 and 0.4 $R_\odot$ for the 9.8 and 87 day periods, respectively. Assuming a constant effective temperature and a radius of 63 $R_\odot$ results in photometric amplitudes in the range 0.002–0.01 mag. If nonradial pulsations were present, then this value should be smaller. The estimates are well below the detection limits of the photometric measurements by Percy & Welch (1981).

Unfortunately, the data are too sparse to search for other periods shorter than the 87 day period. Such short-term variability may account for much of the "noise" in the data periodogram (Fig. 2). If both short- and long-term variability are present in α Per, then the RV behavior for this star may be closely related to the variability seen in K giant stars, which show variations on a variety of timescales (Hatzes & Cochran 1993, 1994a).

Regardless of whether the 87 day or 9.8 day period is indeed present it seems that stellar pulsations are a very likely explanation for the RV variations of α Per. Figure 10 shows the approximate location of the Cepheid instability strip in the H-R diagram. The blue edge is the theoretical one derived by Iben & Tuggle (1975), while the red edge is taken from Fernie (1990), who placed it redward of the coolest known Cepheid. Also shown are the locations of α Per, Polaris (= α UMi), and γ Cyg. Alpha Per may be a pulsating star outside of the instability strip. If so, then the instability strip may extend to hotter temperatures than theoretical calculations indicate. One intriguing possibility is that α Per is just entering or leaving the instability strip. If so, then continued monitoring of this star with precise RV techniques in the ensuing years may show noticeable changes in the pulsational amplitude. Finding more examples of such low-amplitude pulsations outside the instability strip may better define the boundaries of this feature as well as discern changes in the pulsational characteristics among stars in different locations with respect to the traditional instability strip boundaries.

The authors wish to thank Gordon Walker for useful comments on an earlier draft of the paper. This research was funded by NSF grant AST 90-17368, support we gratefully acknowledge.

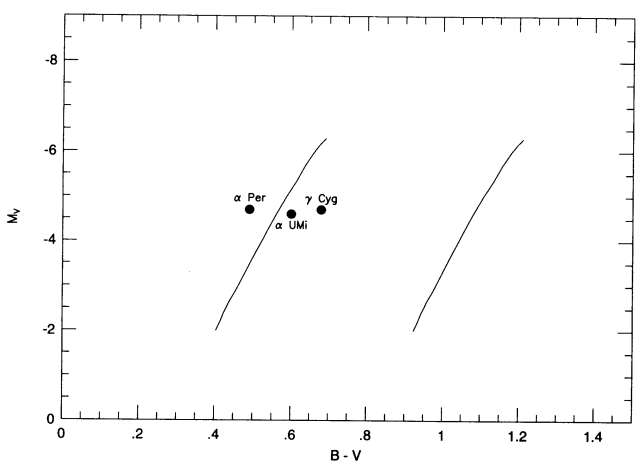

FIG. 10.—Approximate location of the instability strip in the H-R diagram. The blue edge is the theoretical one determined by Iben & Tuggle (1975), and the red edge is the empirical one from Fernie (1990). Also shown are the locations of α Per (HR 1017) and γ Cyg (HR 7796) using the M_V and $B-V$ vaues listed by Humphreys (1978) and Allen (1973).

REFERENCES

Allen, C. W. 1973, Astrophysical Quantities (London: Athlone)
Antonello, E., Mantegazza, L., & Poretti, E. 1986, A&A, 159, 269
Butler, R. P. 1992, ApJ, 394, L25
Cochran, W. D., & Hatzes, A. P. 1994, Ap&SS, 212, 281
Danzinger, I. J., & Faber, S. M. 1972, A&A, 18, 428
Dinshaw, N., Matthews, M., Walker, G. A. H., & Hill, G. M. 1989, AJ, 98, 2249
Eggen, O. J. 1985a, AJ, 90, 1260
———. 1985b, AJ, 90, 1278
Fernie, J. D. 1976, PASP, 88, 116
———. 1990, ApJ, 354, 295
Fernie, J. D., & Hube, J. O. 1971, ApJ, 168, 437
Harris, G. L. H. 1976, ApJS, 30, 451
Hatzes, A. P., & Cochran, W. D. 1993, ApJ, 413, 339
———. 1994a, ApJ, 422, 366
———. 1994b, ApJ, 432, 763
Humphreys, R. M. 1978, ApJS, 38, 309
Iben, I., & Tuggle, R. 1975, ApJ, 197, 39
Kraft, R. P. 1961, ApJ, 134, 616
Kurucz, R. L. 1979, ApJS, 40, 1
Libbrecht, K. G. 1988, ApJ, L51
Marcy, G. W., & Butler, R. P. 1992, PASP, 104
Parsons, S. B., & Bouw, G. D. 1971, MNRAS, 152, 133
Percy, J. R. 1975, Inf. Bull. Variable Stars, 983
Percy, J. R., Baskerville, I., & Trevorrow, D. W. 1979, PASP, 91, 368
Percy, J. R., & Welch, D. L. 1981, PASP, 93, 367
Roberts, D. H., Lehár, J., & Dreher, J. W. 1987, AJ, 93, 968
Scargle, J. D. 1982, ApJ, 263, 835
Smith, P. H., McMillan, R. S., & Merline, W. J. 1987, ApJ, 317, L79
Walker, G. A. H., Yang, S., Campbell, B., & Irwin, A. W. 1989, ApJ, 343, L21